

Supporting Information

In-situ TEM investigation of congruent phase transition and structural evolution of nanostructured silicon/carbon anode for lithium ion batteries

Chong-Min Wang^{1*}, Xiaolin Li², Zhiguo Wang², Wu Xu³, Jun Liu², Fei Gao^{2*}, Libor Kovarik¹, Ji-Guang Zhang³, Jane Howe⁴, David J. Burton⁵, Zhongyi Liu⁶, Xingcheng Xiao⁷, Suntharampillai Thevuthasan¹, and Donald R. Baer¹

¹ Environmental Molecular Sciences Laboratory, Pacific Northwest National Laboratory, Richland, WA 99352, USA

² Fundamental and Computational Science Directorate, Pacific Northwest National Laboratory, Richland, WA 99352, USA

³ Energy and Environmental Directorate, Pacific Northwest National Laboratory, Richland, WA 99352, USA

⁴ Oak Ridge National Laboratory, Oak Ridge, TN 37831-6064, USA

⁵ Applied Sciences, Inc., Cedarville, OH 45014-0579, USA

⁶ Electrochemical Energy Research Laboratory, General Motors Global R&D Center, Warren, MI 48090, USA

⁷ Chemical Sciences and Materials Systems Laboratory, General Motors Global R&D Center, Warren, MI 48090, USA

This on-line supporting information includes the following content:

1: Supporting Online Movies:

2: Density function theory molecular dynamic calculations:

3: Additional Figures:

Figure S1: STEM-HAADF image and EDS line profile of Si showing that for this a-Si-CNF the Si is coated at both the outside and inside of the CNF.

Figure S2: Matching of the experimental diffraction pattern with the calculated one for Li₁₅Si₄.

* Authors to whom all correspondence should be addressed: Chongmin.Wang@pnnl.gov

Fei.Gao@pnnl.gov

1: Supporting Online Movies:

Movie S1: An in-situ TEM movie showing the initial charging of an a-Si-CNF. This movie features the formation of amorphous Li_xSi during the charging of the a-Si-CNF. Note the sequential propagation of the reaction front as evidenced by the thickening of the coating layer. To clearly visualize the reaction propagation, this movie is played at a speed of 10 frames per second.

Movie S2: An in-situ movie showing a charge-discharge cycle of an a-Si-CNF. This movie features (1) the conversion of a-Si to Li_xSi when charged; (2) subsequent crystallization of amorphous Li_xSi to crystalline $\text{Li}_{15}\text{Si}_4$ and the crystallization process is directly visible from the change of the diffraction contrast upon the formation of the crystalline phase; (3) upon discharging, the crystalline $\text{Li}_{15}\text{Si}_4$ reversibly transform to amorphous Li_xSi and eventually amorphous Si. Note that the crystallization is uniform and leads to no phase separation, indicating this crystallization is a congruent process. This movie is played at speed of 80 frames per second.

Movie S3: An in-situ movie (left panel is the image and the right panel is the diffraction pattern) showing the formation of a- Li_xSi during the charging, which is accompanied by the gelation of the electrolyte wetting layer by the electron beam. This gelled electrolyte layer is amorphous and covers the a- Li_xSi layer. The a- Li_xSi crystallizes to $\text{Li}_{15}\text{Si}_4$, while the gelled electrolyte remains as amorphous as revealed by the diffraction contrast in the image as well as the diffraction pattern.

Movie S4: An in-situ movie (left panel is the image and the right panel is the diffraction pattern) showing the separation between the gelled amorphous electrolyte layer and a- Li_xSi during the discharging. Note the transition from crystalline $\text{Li}_{15}\text{Si}_4$ to amorphous phase during the discharging as indicated by the diffraction contrast as well as the disappearance of the diffraction spots on the diffraction pattern. This observation clearly demonstrates the bonding between the a- Li_xSi and CNF is stronger than that between a- Li_xSi and the gelled electrolyte.

Movie S5: An in-situ movie showing the structural evolution during the re-charging of the discharged wire as shown in Movie S4. Note the gap between the gelled amorphous electrolyte layer and a-Si formed during the discharging is fully filled following the re-charging, demonstrating the reversible charge-discharge.

2: Density function theory molecular dynamic calculations:

All the calculations were performed using density functional theory, within local density approximation¹ using the Ceperly-Alder parameterization as implemented in the SIESTA code², which adopts a linear combination of numerical localized atomic orbital basis sets for the description of valence electrons and norm-conserving nonlocal pseudopotentials for the atomic core³. The valence electron wave functions were expanded by using double- ζ basis set. The charge density was projected on a real space grid with a cutoff of 120 Ry to calculate the self-consistent Hamiltonian matrix elements.

The crystalline alloys are constructed from the crystalline structure database and experimental results. The amorphous structures were prepared by using the melt quenching method with density functional theory molecular dynamics simulations. We equilibrate the system at temperature 4000 K at least for 5 ps (5000 MD steps with a time step of 1 fs), which is above the melting point. We then quickly quenched the systems to ~ 0 K and the lattices were further

relaxed together with the atomic coordinates using the conjugate gradient minimization. Large systems were used to model the amorphous structure. The numbers of atoms used for the $E_{\text{Li}x\text{Si}}$ alloys are: LiSi (192/192), $\text{Li}_{12}\text{Si}_7$ (192/112), $\text{Li}_{13}\text{Si}_4$ (208/64), $\text{Li}_{15}\text{Si}_4$ (240/64), $\text{Li}_{21}\text{Si}_5$ (336/80), and $\text{Li}_{22}\text{Si}_5$ (352/80)

References

- (1) Ceperley, D. M.; Alder, B. J. *Phys. Rev. Lett.* **1980**, *45*, 566.
- (2) Soler, J. M.; Artacho, E.; Gale, J. D.; Garcia, A.; Junquera, J.; Ordejon, P.; Sanchez-Portal, D. *J. Phys.-Condens. Matter* **2002**, *14*, 2745.
- (3) Troullier, N.; Martins, J. L. *Phys. Rev. B* **1991**, *43*, 1993.

3: Additional Figures:

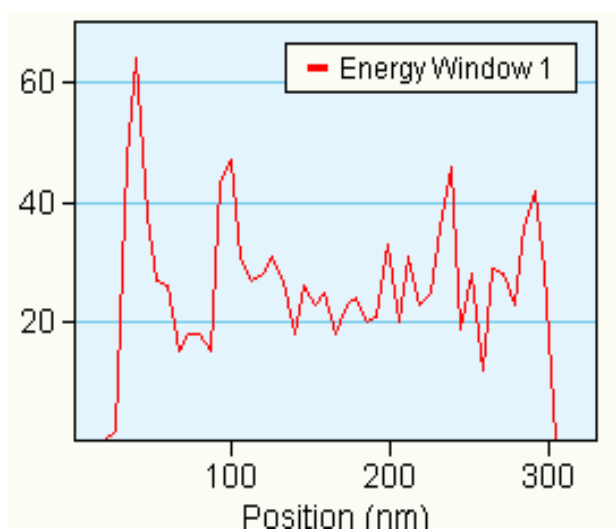
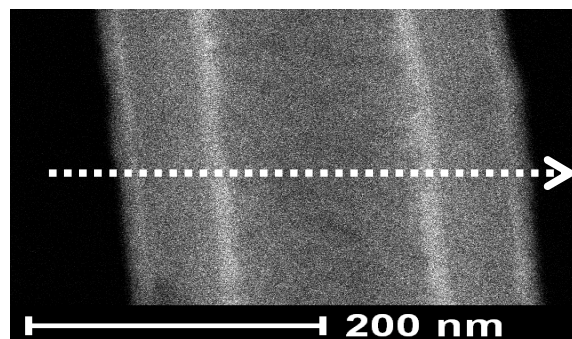


Figure S1: STEM-HAADF image and EDS line profile showing that for some CNF the Si is coated at both the outside and inside of the tube.

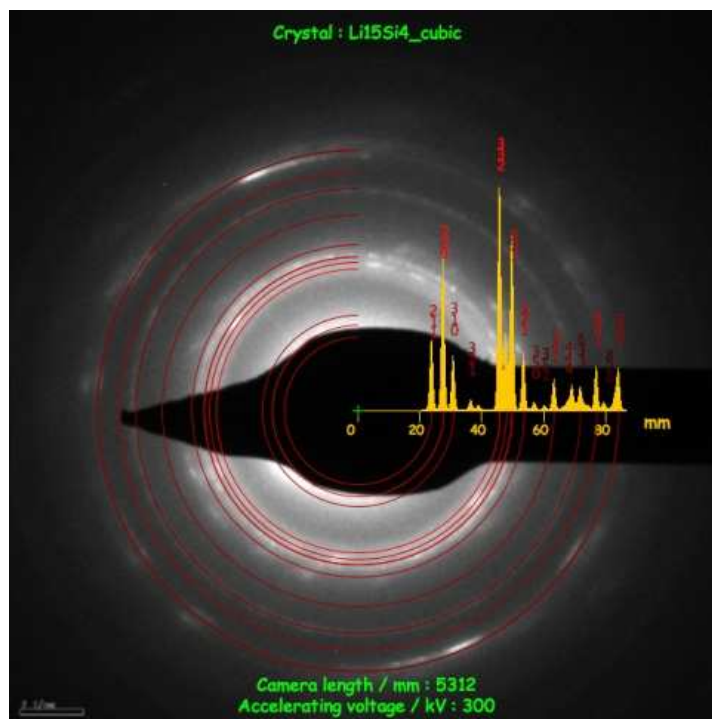


Figure S2: Matching of the experimental diffraction pattern with the calculated one for $\text{Li}_{15}\text{Si}_4$.